The relative roles of feedforward and feedback in the control of rhythmic movements

ARTHUR D. KUO

Dept. Mechanical Engineering, University of Michigan, Ann Arbor, MI 48109-2125 USA

artkuo@umich.edu   fax: +1 734 647-3170   phone: +1 734 647-2505

Abstract. We use a simple pendulum model to study how the combination of feedforward and feedback can be combined to control rhythmic limb movements. We show that a purely feedforward central pattern generator (CPG) is highly sensitive to unexpected disturbances. Pure feedback control analogous to reflex pathways can compensate for disturbances, but is sensitive to imperfect sensors. We demonstrate that for systems subject to both unexpected disturbances and sensor noise, a combination of feedforward and feedback can improve performance. This combination is achieved by using a state estimation interpretation, in which a neural oscillator acts as an internal model of limb motion that predicts the state of the limb, and by using α-γ coactivation or its equivalent to generate a sensory error signal that is fed back to entrain the neural oscillator. Such a hybrid feedforward/feedback system can optimally compensate for both disturbances and sensor noise, yet it can also produce fictive locomotion when sensory output is removed, as is observed biologically. CPG behavior arises due to the interaction of the internal model and a feedback control that uses the predicted state. We propose an interpretation of the neural oscillator as a filter for processing sensory information rather than as a generator of commands.

Abbreviations: CPG, central pattern generator; FF, feedforward; FB, feedback; HFB, hybrid feedforward / feedback; rms, root-mean-square

Key Words: central pattern generator, locomotion, reflexes, motor control, efference copy

1 Introduction

Central pattern generators (CPGs) are neural circuits that generate periodic motor commands for rhythmic movements such as locomotion (see Fig. 1a). Although the anatomical details of CPGs are known for only a few cases, the motor commands have been shown to originate from the spinal cords of a variety of vertebrates (Grillner and Wallén, 1985). These circuits can function *in vitro* even when isolated from the brain, as evidenced by locomotion in decerebrate cats (Shik et al., 1966); and when isolated from the motor and sensory apparatus of the limbs (Grillner and Wallén, 1985). Fictive locomotion also occurs in invertebrates (Pearson and Fourtner, 1975). Locomotor CPGs were originally thought to entrain the limbs to oscillate at a sustained frequency, providing a rhythmic motor command to overcome dissipation associated with friction and other phenomena (Brown, 1914). However, the existence of limb dynamics and of feedback pathways may lead to a different interpretation of CPG activity.

The limbs, which receive commands from CPGs, have natural dynamics that govern many aspects of locomotion. In walking, the motion of the limbs has been likened to that of coupled pendula, so that there is a periodic exchange between potential and kinetic energy. In running, the legs function in a manner analogous to springs, with the exchange occurring between kinetic energy of the center of mass and the potential energy of the springs (Alexander, 1989). For both of these cases, the dynamics are sufficiently significant that they govern many aspects of locomotion. Timing, limb kinematics, and ground reaction forces can all be predicted to a surprising degree of fidelity through consideration of dynamics alone (McGeer, 1993), without regard to the commands arising from CPGs. In fact, the resonant limb dynamics might limit the influence of CPG function to a greater degree than the converse. For example, humans scale walking speed primarily by adjusting step amplitude and stance duration; swing phase duration is closely tied to the pendulum-like motion of the legs, making it energetically costly to tune away from what is natural (Alexander, 1989; Kuo, 2001).

From a control perspective, motion of a system whose mechanics dictate a need for efficiency and stability is better accomplished with feedback, as opposed to pure feedforward signals. The limbs, having a natural rhythmic state, can act as a peripheral pattern generator that triggers the feedback signals necessary to supply energy and sustain oscillatory behavior (Fig. 1b; see also Gray, 1950). In fact, nearly all existing examples of physical robots that locomote and have significant dynamics are based on feedback control (e.g., Raibert, 1986). The combination of natural dynamics and feedback signals produces motion without need for a centrally generated command. Practically speaking, feedback is advantageous because limbs do not generally behave exactly as commanded
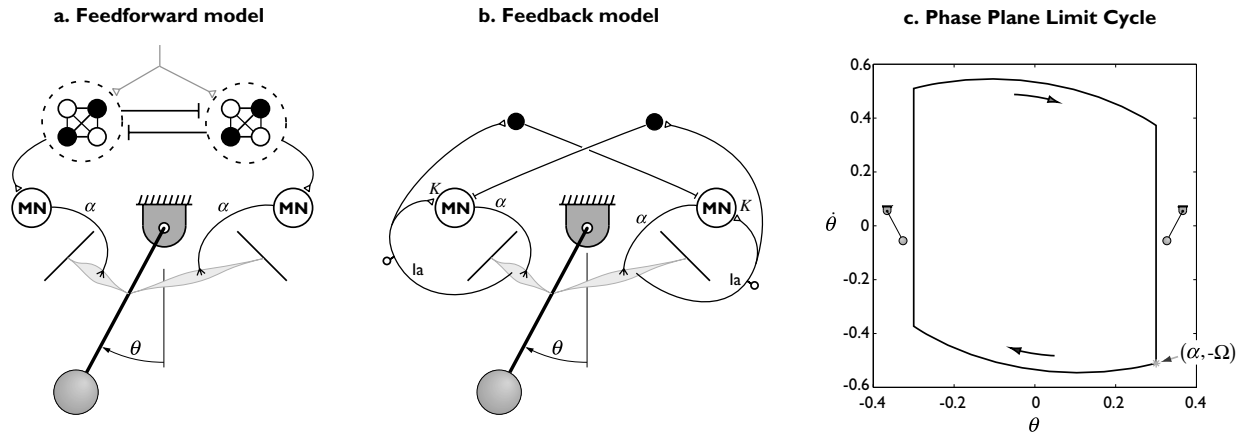
a. Feedforward model **b. Feedback model** **c. Phase Plane Limit Cycle**

Fig. 1. Pure feedforward and feedback circuits for rhythmic movements. **a.** Feedforward system is driven by two mutually inhibitory half-centers (enclosed by dashed circles) which produce alternating bursts of activity driving motor neurons (MN). Muscles, triggered by α motor activity, produce motion of a limb. Half-centers receive tonic excitation, and appear to comprise multiple neurons, and may include nonspiking neurons. **b.** Feedback system also produces rhythmic movement, but only through feedback of muscle stretch sensation through Ia afferents, which trigger monosynaptic reflex commands and contralateral inhibition. If gain K is properly tuned, system will exhibit limit cycle behavior. **c.** Identical limit cycles, shown here in a phase plane plot, can be generated through pure feedforward or feedback. Limit cycle shown is for parameters $\alpha = 0.3$, $\zeta = 0.1$.

(Hatsopoulos, 1996), and a feedback signal can compensate for unexpected disturbances. A centrally generated command does not, by definition, respond to sensory information, and performance can potentially suffer if disturbances are significant.

Biological evidence demonstrates that feedback pathways do in fact act in concert with CPGs. For example, feedback circuits in the lamprey can entrain the CPG to physical motion (Grillner et al., 1981). Cohen (1992) has emphasized that there is a two-way interaction between the CPG and the body, in which the CPG actively processes sensory inputs and mechanical factors contribute to entrainment of the CPG. Given the coexistence of both feedforward and feedback and engineering evidence favoring feedback alone, we ask what possible advantage there might be to this combination.

Modern control theory provides a basis for studying the roles of feedforward and feedback. Control theory acknowledges the superiority of feedback for control of systems that are subject to unexpected disturbances. However, feedback is predicated on the ability to correctly sense the state of the system to be controlled. Because sensors are not perfectly accurate in practice, there arises a need to make use of imperfect sensory information to generate the appropriate feedback command. The results of Kalman show that an optimal estimate of the system state can be produced using an internal model to predict the expected state and associated sensory output (Bryson and Ho, 1975). The sensory prediction error can then be used to adjust the expected state in an optimal manner, and this estimate can in turn be used to produce the appropriate feedback command. If the internal model is of a system with rhythmic behavior, as in locomotion, then the model

will act as a central pattern generator, albeit one which is tuned with sensory feedback. The relative roles of feedforward and feedback should therefore be dependent on the relative significance of unexpected disturbances and imperfect sensors.

In this paper, a simple model will demonstrate these principles. The model is of a damped pendulum driven to oscillate in a manner analogous to limb motion. We first show that for an ideal system, either feedforward or feedback control can be used to produce the desired oscillation. However, in the presence of unexpected disturbances, the pure feedforward control has significant performance disadvantages. We then show that the pure feedback system also has performance disadvantages when sensory information is imperfect. An optimally designed intermediate of the two extremes performs best when both types of disturbances are present. These results lead to a new interpretation in which CPGs generate oscillatory signals more to assist the decoding of sensory information rather than to produce feedforward motor commands. Lastly, we will discuss some physiological implications of this interpretation.

2 Pendulum Model

As a simple model for a limb undergoing rhythmic motion, we will employ a simple damped pendulum under the influence of either gravity or a torsional spring (or any combination of the two), forced to oscillate about vertical equilibrium by impulsive torques applied at the extremes of motion. The impulsive torques are a mathematical convenience that approximate the influence of short bursts of muscular

activity. Assuming small angles, the linearized equation of motion for the pendulum will be used:

$$\ddot{\theta} + 2\zeta\dot{\theta} + \theta = u \qquad (1)$$

where θ is the angle of the pendulum as measured counterclockwise from the vertical, ζ is the damping ratio, and u is the externally applied torque. We will employ normalized units in the subsequent analysis, with mass in units of pendulum mass m, length in units of pendulum length ℓ. Time is in units of $1/\omega_n$, with the definition of ω_n depending on the influence of gravity or spring-like muscles. If gravitational potential energy is significant, $\omega_n \triangleq (g/\ell)^{1/2}$. The resonant frequency ω_n may also be modified to include a spring constant if spring-like potential energy is significant. There is a direct equivalence between a model with impulsive torques and one with spring-like muscles acting over an arbitrary duty factor (see Appendix A of Kuo, 2001).

The pendulum is to undergo steady-state oscillations of amplitude α and with initial angular velocity $\dot{\theta}$ of magnitude Ω in units of ω_n (see Fig. 1c). We therefore define the initial condition

$$\theta(0) = \alpha, \ \dot{\theta}(0) = -\Omega. \qquad (2)$$

The damping ratio ζ determines how much speed is lost during one half-period, crudely modeling the energy loss due to dissipatory effects, which can occur both continuously, as with friction, and at discrete instances, as during foot contact in animal locomotion. We define the constant η to describe the amount of speed retained by the end of each half-period of duration τ, after which the speed Ω will be restored instantaneously through application of an instantaneous impulse. We will restrict allowable behaviors to those with non-negative η. Employing the '−' superscript to denote conditions just prior to the impulse, and '+' for just after, the half-period condition is

$$\theta(\tau^-) = -\alpha, \ \dot{\theta}(\tau^-) = -\Omega\eta. \qquad (3)$$

At time τ an impulse

$$I = \int_{\tau-}^{\tau+} u(t)dt \qquad (4)$$

is applied. In order for the pendulum to exhibit periodic behavior, it is necessary that this impulse results in the initial condition for the next half-period,

$$\theta(\tau^+) = -\alpha, \ \dot{\theta}(\tau^+) = \Omega, \qquad (5)$$

which in turn ends when the pendulum returns to its original position of (2). The amplitude of swing and half-period τ determine the dimensionless speed

$$U \equiv \frac{2\alpha}{\tau}. \qquad (6)$$

To restrict the number of free parameters, the pendulum boundary conditions will be restricted to those corresponding to a constant speed $U = 0.5$, which is the speed of an undamped pendulum swinging freely with amplitude $\pi/4$. This constraint, along with (1) and (2), make τ and Ω functions of two free parameters α and ζ. Note that limit cycles for other speeds may be found by scaling appropriate trajectories at the nominal speed, due to the linearity of the pendulum dynamics.

The following free parameter values are chosen for the nominal limit cycle (Fig. 1c): $\alpha = 0.3$ rad, $\zeta = 0.1$. At a speed of $U = 0.5$, this results in a half-period of $\tau = 1.2$, initial velocity of magnitude $\Omega = 0.510$ and loss constant $\eta = 0.731$. Although the model only produces rhythmic limb motions, the parameter set is chosen to roughly correspond to leg swinging in freely selected human walking at 1.5 m/s and 2.5 Hz, although in humans much of the energy loss occurs at heel contact rather than being distributed over an entire stride as is the case here (Donelan et al., 2001; Alexander, 1989).

3 Feedforward and Feedback Systems

3.1 Feedforward and Feedback Control Laws

In the absence of disturbances, identical limit cycles may be obtained using any combination of feedforward and feedback. A pure feedforward control applies the impulses at every half-period, regardless of the pendulum's state (see Fig. 1a). The control law is, from (3)-(5),

$$\textbf{FF}: \ I(t) = \begin{cases} \Omega(1+\eta) & \text{if } t = (2k-1)\tau \\ -\Omega(1+\eta) & \text{if } t = 2k\tau \end{cases}, \ k = 1, 2, 3\ldots (7)$$

The asymptotic stability of this system may be verified through application of Poincare maps (Guckenheimer & Holmes, 1983).

A pure feedback, however, applies the impulses as a function only of state (i.e., the pendulum's position and velocity) and not explicitly of time (see Fig. 1b). One possible feedback law is

$$\textbf{FB}: \ I(\theta, \dot{\theta}) = -\text{sgn}(\theta)(1+\eta)\Omega - K(\dot{\theta} - \text{sgn}(\theta)\eta\Omega)$$
$$\text{if } \theta = \pm\alpha \text{ or } \dot{\theta} = 0 \qquad (8)$$

where K is a control feedback gain, and the bounds on limb motion α and angular rate Ω are specified by a higher-level (descending) command. The first term

above is equal to the nominal impulse applied by the FF control law, and the second term is a corrective impulse dependent on the deviation of $\dot{\theta}$ from the nominal. When $K = 1$, which will be taken as the default case, the FB control law applies an exactly corrective impulse at each extreme of motion. If the pendulum does not have sufficient energy to reach $\theta = \pm\alpha$, an impulse is supplied to redirect it toward one of these limits starting from zero velocity. In principle, a feedback law could alternatively supply an exactly corrective impulse when $\dot{\theta} = 0$, but the calculation of the appropriate magnitude cannot, in general, be solved analytically. It may be verified that the FB control law provides global stability.

The pure feedforward and feedback control laws differ in behavior only when disturbances act on the system. We will consider two types of disturbances: those that apply unexpected torques w, and those that add unexpected errors v to measurements of the state. Equation (1) is therefore replaced by

$$\ddot{\theta} + 2\zeta\dot{\theta} + \theta = u + w \tag{9}$$

and the feedback law FB (8) is made a function of *measured* states

$$\theta_m = \theta + v_1, \ \dot{\theta}_m = \dot{\theta} + v_2 \tag{10}$$

rather than actual states. To characterize average behavior, the disturbances w, v_1, and v_2, may be modeled as noise with short correlation time, as described below.

The feedforward and feedback systems also differ in analytical tractability. The FF control is a periodic excitation of a linear system, for which analytical solutions can be found. In contrast, the FB control law is neither continuous nor periodic—it uses discrete impulses with triggering time and magnitude both functions of the state—and does admit analytical solutions. Simulations were therefore used to characterize the behaviors for both systems, and FF

results were verified against analytical predictions.

3.2 Sensitivity to Disturbances and Measurement Noise

We will use the pendulum system to demonstrate two fundamental control principles: that pure feedforward systems are sensitive to unexpected disturbances, and pure feedback systems are sensitive to measurement errors. We first apply a 10% perturbation to the initial velocity, which results in oscillatory behavior of the pendulum under FF control, as shown in Fig. 2. To describe this behavior, we compute errors in θ and $\dot{\theta}$ from the nominal values directly after each impulse following the initial release. The FF system produces a maximum error of 14.1% in θ before slowly converging to the limit cycle. Settling time, defined as the number of half-periods required for error to go below 5%, is 10 half-periods for θ and 6 half-periods for $\dot{\theta}$. To demonstrate the sensitivity on parameter values, the maximum θ errors were computed for a range of values for α and ζ (see Fig. 2b). The parameter domain was for amplitudes between 0 and $\pi/4$, and ζ between 0 and 1.2. Large errors, 20% and above, were found for values of α less than approximately 0.2, and errors on the order of 10% were found for values of α up to approximately 0.4. These and subsequent results were computed using a model implemented in Simulink 2 (The MathWorks Inc., Natick, MA). The limit cycle behavior was computed using numerical integration by Simulink's ode23 variable step size function. The relative integration error tolerance was 1e-3, and the absolute tolerance was 1e-6.

The FB system, using $K = 1$, performs considerably better under the same conditions, assuming accurate measurements of the state (i.e., $v_1 = 0$, $v_2 = 0$). Following initial release, the control law supplies an exactly corrective impulse, so that the maximum error

Fig. 2. Feedforward systems are sensitive to unexpected disturbances. **a.** When feedforward system of Fig. 1a is started with an initial velocity with 10% error, system exhibits oscillatory behavior and slow convergence to limit cycle. **b.** Maximum position error due to 10% initial velocity perturbation, as a function of parameters α (amplitude) and ζ (damping ratio). Domain is restricted to parameter values for which pendulum has no overshoot, delimited by zero velocity boundary. Note that majority of parameter values result in greater than 10% position error, demonstrating high sensitivity to perturbations.
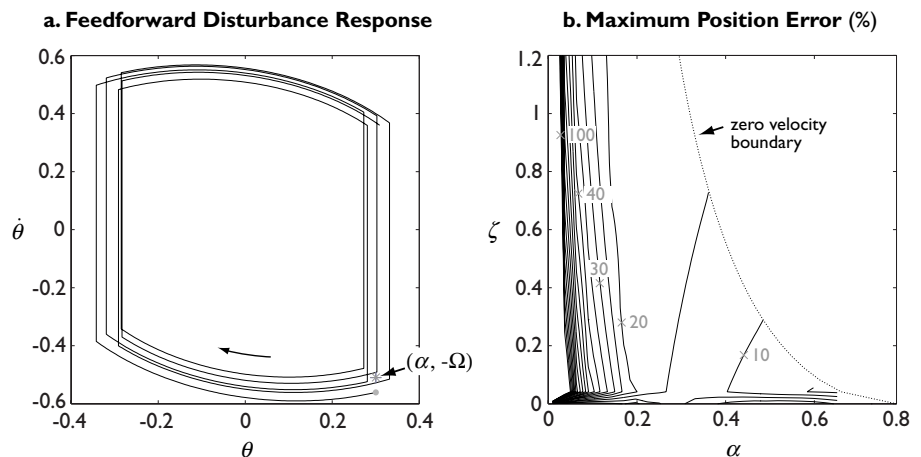

a. Feedforward Disturbance Response

b. Maximum Position Error (%)

Fig. 3. Feedback systems are sensitive to measurement errors. **a.** When feedback system of Fig. 1b is subject to noise-like errors in measurements of θ and $\dot{\theta}$, system exhibits continual oscillations about limit cycle. **b.** Steady-state position error, shown as percentage rms (root-mean-square), as a function of parameters α (amplitude) and ζ (damping ratio). Feedback system exhibits sensitivity to measurement errors for low amplitude movements.

a. Feedback Measurement Noise Response

b. Steady-State Position Error (% rms)
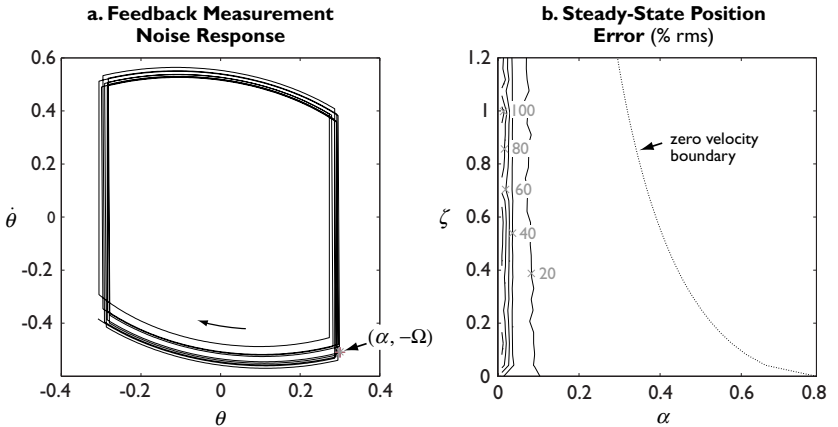
is 0% and the settling time is 1 half-period for both θ and $\dot{\theta}$. This behavior is invariant to parameter choice, and is more similar to perturbation responses seen in animals (e.g., Mellen et al., 1995).

However, the FB system does not perform as well when measurements are imperfect. To assess sensitivity to measurement noise, we evaluated steady-state behavior, defined as root-mean-square (rms) errors over 100 steps, with simulated white noise, using noise parameters determined as follows. We assume that the precision of sensory data does not greatly exceed the ability of the motor system to regulate movement and vice versa, implying that measurement noise should be approximately equivalent to the variability due to disturbance noise alone. First, nominal disturbance noise w with zero mean and arbitrarily chosen covariance $(0.2\Omega\omega_n)^2$, and no measurement noise, was applied to the FF system. This value produced steady-state root-mean-square errors of 7.2% in θ and 4.7% in $\dot{\theta}$. Root-mean-square error was computed at discrete instances, based on the deviations of θ and $\dot{\theta}$ from the fixed point directly following each impulse for 100 half-periods. These errors were used to determine nominal measurement noise characteristics: v_1 and v_2 had zero mean and variances equal to the steady-state disturbance noise response. In other words, v_1 and v_2 had rms values of 7.2% and 4.7%, respectively. For computations, band-limited white noise was simulated with normally distributed random numbers applied in discrete time with a zero-order hold and a step size 40 times smaller than the half-period τ.

When the FB system operates with no disturbance noise but with nominal measurement noise as described above, the state oscillates about the fixed point (see Fig. 3a). The steady-state rms errors are 5.0% for θ, and 4.5% for $\dot{\theta}$. Performing the same calculations for a range of parameter values for α and ζ (Fig. 3b), but with identical noise attributes, we find that the FB

system grows increasingly sensitive to measurement noise inversely proportional to α, because error is reported as a percentage. In terms of absolute error, the FB system is insensitive to parameter choice.

In contrast, the FF system is completely insensitive to measurement noise, because impulses are applied according to an intrinsically generated rhythm rather than sensory measurements.

4 Hybrid Feedforward/Feedback System

Given the respective weaknesses of both FF and FB and the likely presence of both unexpected disturbances and sensory measurement errors in any biological system, we next explore whether there is some advantage to be gained by combining FF and FB. To this end, we desire a model which can act as a pure FF or FB system at the extremes, but which mixes the two in some flexible manner. Moreover, the hybrid model should exhibit the ability to intrinsically generate motor activity even in the absence of sensory feedback, as is observed in CPGs. After developing such a model, we will apply both types of noise and examine its behavior as the FF/FB mixture is varied, using optimal state estimation theory as a parameterization tool.

4.1 Hybrid Feedforward/Feedback Model

A hybrid model satisfying these requirements is obtained by modifying the FF system to incorporate elements of the FB system (see Fig. 4). First, the CPG oscillators will be assumed to model the dynamics of the pendulum, producing a prediction of motion that in turn drives the FB system. Second, we adopt the equivalent of α-γ coactivation so that the sensors, in this case muscle stretch receptors, signal deviations from the commanded movement, i.e., unexpected disturbances. Third, the resulting error signals are fed back to the half-center oscillators with a CPG feedback
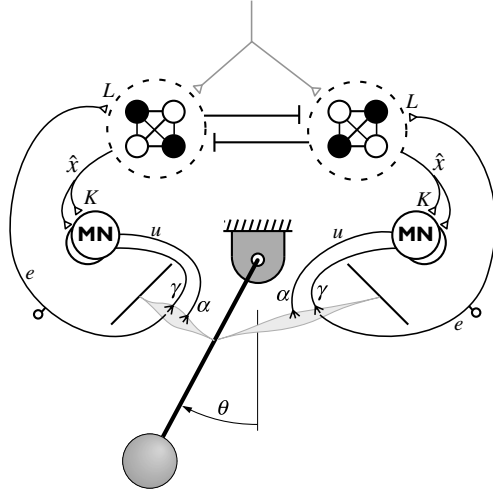
Hybrid FF/FB model

Fig. 4. Hybrid system combines feedforward (FF) and feedback (FB) in such a way that limit cycle behavior is retained. Half-centers (enclosed by dashed circles) produce bursts of α-γ co-activation with control gain K. Coactivation causes stretch receptors to adjust sensitivity so that afferents feed back error information e, signaling unexpected disturbances. Error feedback entrains half-center oscillators with gain L, referred to as *CPG feedback gain*. When L is zero, error information is ignored and system functions identically to pure FF system of Fig. 1a. When L is very large, half-centers are immediately entrained to error signals, essentially acting as relay interneurons, and system behaves identically to pure FB system of Fig. 1b. (When L is sufficiently large, interneurons are largely redundant and can be bypassed, resulting in identical topology of pure FB system.) For any value of L, hybrid system produces invariant limit cycle, though with varying degrees of sensitivity to unexpected disturbances and measurement errors. When feedback e is eliminated, half-center oscillators produce nominal limit cycle behavior, regardless of magnitude of L.

gain L (not to be confused with the *control* feedback gain K), which entrains the FF component to actual movement. The oscillator output in turn triggers the reversing torque that in the FB system would be triggered directly by the sensed leg angle (8). The CPG feedback gain may be varied between 0, in which case behavior identical to the FF system is achieved, and values approaching infinity, causing the behavior to approach that of the FB system.

Mathematical implementation of the hybrid model is most conveniently performed in state space. Defining the vectors and system matrices

$$x \equiv \begin{bmatrix} \theta \\ \dot{\theta} \end{bmatrix}, \quad y \equiv \begin{bmatrix} \theta_m \\ \dot{\theta}_m \end{bmatrix}, \quad w' \equiv \begin{bmatrix} w \\ w_2 \end{bmatrix}, \quad A \equiv \begin{bmatrix} 0 & 1 \\ -1 & -2\zeta \end{bmatrix},$$

$$B \equiv \begin{bmatrix} 0 \\ 1 \end{bmatrix}, \quad \Gamma \equiv \begin{bmatrix} 0 & 1 \\ 1 & 0 \end{bmatrix}$$

the state-space equivalents to (9) and (10) are

$$\dot{x} = Ax + Bu + \Gamma w' \qquad (11)$$

$$y = x + v. \qquad (12)$$

Note one difference with the former system: the disturbance vector w' has been expanded to include an additional component w_2 that affects $\dot{\theta}$ through Γ.

We assume that the CPG oscillators, as a group, exhibit separate but identical dynamics to the body, but possibly different inputs. The CPG's intrinsic state will be referred to as $\hat{x}$, so that its dynamics are described by

$$\dot{\hat{x}} = A\hat{x} + Bu - Le \qquad (13)$$

$$e = \hat{x} - y. \qquad (14)$$

These equations reflect the fact that the CPG does not have access to values for unexpected disturbances and measurement noise. Even the feedback information it receives regarding limb position or velocity are ambiguous due to the interaction of γ input to the muscle spindles. Finally, a hybrid control $u = f(\hat{x})$ is constructed by applying the FB control law to the intrinsic state:

HFB: $I(\hat{x}) = -\text{sgn}(\dot{\hat{\theta}})(1+\eta)\Omega - K\left(\dot{\hat{\theta}} - \text{sgn}(\dot{\hat{\theta}})\eta\Omega \right)$

$$\text{if } \hat{\theta} = \pm\alpha \text{ or } \dot{\hat{\theta}} = 0. \qquad (15)$$

The model described by (13) and (14) produces rhythmic limb motion based on feedback only of sensory error e. It is able to do so because the internal model generates the expected limb motion, and requires updates only to correct for errors in that expectation, relayed by e. We therefore interpret muscle spindle output as a comparison between actual and expected limb motion, effectively providing feedback of e.

The model also satisfies all requirements for the hybrid system. When L is the zero matrix (2×2), the impulses are applied at intervals of τ, just as in the FF system. Elimination of feedback e has the same effect. It may also be verified that for large values of L_{11} and L_{22} the intrinsic state simply follows the measured state.

To complete the analysis, it is necessary to prescribe a simple parameterization of L such that steady-state behavior in the presence of disturbances and measurement errors may be evaluated over a range of values between the FF and FB extremes. The next section introduces a parameterization based on a single index that determines all four entries of L.

4.2 Optimal State Estimation Theory

The preceding development lends itself well to analysis by optimal state estimation theory, which is concerned with the determination of a system's state

based on measurements which are indirect, imperfect, or ambiguous. This theory can be used to interpret CPG behavior as optimal in some sense, although the primary reason driving its application is simply as a means to parameterize the CPG feedback gain.

An optimal estimate of the state of a linear, time-invariant system may be obtained by using an internal model of the system to predict both the state and the associated sensory output. The estimation error may be minimized in the mean-square sense by feeding back the sensory prediction error to the internal model using gains which are constant in the steady-state condition (Bryson and Ho, 1975).

Our hybrid system uses a single parameter, the *CPG feedback index* (CFI), to set the relative contributions of feedforward vs. feedback. The CFI is employed in the design equations for the optimal estimator as follows:

$$AP + PA^T - PV^{-1}P + 10^{CFI} \cdot \Gamma W \Gamma^T = 0 \qquad (16)$$

$$L = PV^{-1} \qquad (17)$$

where $W \equiv \text{cov}\, w'$ and $V \equiv \text{cov}\, v$. The estimator gain L depends on the relative magnitudes of W and V, and the CFI inflates the influence of W over V. It may be verified that if W and V are positive definite, then both L_{11} and L_{22} asymptotically approach lines proportional to 10^{CFI} as CFI grows in the negative direction, and both asymptotically approach lines proportional to $10^{CFI/2}$ as CFI grows in the positive direction. The off-diagonal entries of L, which couple $\hat{\theta}$ to $\dot{\theta}_m$ and $\hat{\dot{\theta}}$ to θ_m, approach 0 as CFI grows in either direction.

The estimated state is then used as input to the closed-loop feedback (15). Combining (16)-(17) with the HFB system, the CFI can be used to interpolate between pure FF and FB behavior. The resulting performance depends on the interaction between the predicted $\hat{\theta}$ and $\hat{\dot{\theta}}$ and the control feedback. The estimator is theoretically optimal at CFI = 0, but

simulations are needed to evaluate the overall performance because HFB is a nonlinear feedback.

## 4.3 Performance of Hybrid Feedforward/Feedback System

The CPG feedback index is to be used to evaluate performance of systems using various proportions of feedforward and feedback but subject to noise-like disturbances and measurement errors. Performance will be evaluated in terms of % rms error. We first consider performance as a function of the CPG feedback index (CFI) for nominal values of free parameters, after which we will examine how variation of parameters affects results.

In devising the hybrid system model, we introduced a disturbance w_2 acting directly on $\dot{\theta}$. As with the primary disturbance, w_2 is modeled with zero-mean simulated white noise. To ensure that w remains the dominating influence as in the previous example, we set $\text{cov}\, w_2 = 0.001 \text{cov}\, v_2$.

Using the nominal parameter settings, we calculated CPG feedback gains for integer values of the CPG feedback index ranging from –5 to 5. At CFI = 0, $L_{11} = 1.02\omega_n$, $L_{22} = 3.88\omega_n$; for all index values, the off-diagonal terms of L never exceeded 5% of the diagonal terms in magnitude. Simulations were performed for 100 half-periods, and rms errors relative to the fixed point were calculated as described above. Simulations were also performed using pure FF and FB control under the same conditions to serve as limiting cases. The range of CFI feedback indexes was chosen based on the finding at those extremes, the entries in L were sufficiently small or large in magnitude to induce significant errors in finite-precision arithmetic.

Results show that there is a hybrid combination of FF and FB that is least sensitive to the disturbance/measurement noise combination (see Fig. 5). For the noise levels chosen, minimum steady-state

Fig. 5. Steady-state position and velocity errors (bars) and CPG feedback gains (solid lines) for hybrid system subject to noise-like perturbations and measurement errors, as function of *CPG feedback gain index* (CFI), which sets value of CPG feedback gain. Index of 0 corresponds to optimal CPG feedback gain, as calculated from optimal state estimation equations. Negative index values of increasing magnitude correspond to decreasing *L,* approaching pure FF system. Positive index values of increasing magnitude correspond to increasing *L,* approaching pure FB system. **a.** Position errors, in terms of % rms, are minimized for feedback gain index of 0 and is relatively insensitive to excessive CPG feedback. Errors increase over fourfold over minimal value for pure FF and FB systems. Right-hand axis is for gain L_{11}. **b.** Velocity errors, in terms of % rms, are also minimized for index 0. Right-hand axis is for gain L_{22}.
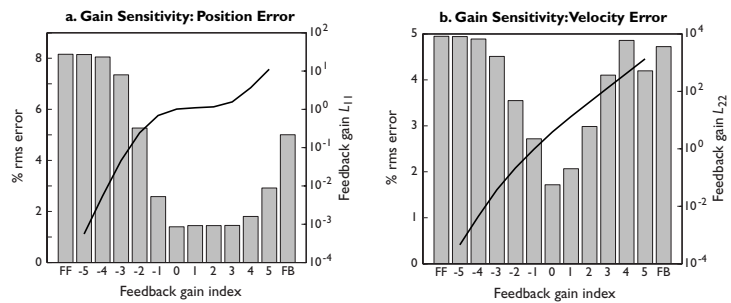
errors were 1.4% rms in θ and 1.7% rms in $\dot{\theta}$, and this minimum was achieved with a CPG feedback index of 0. Errors increased as the CPG feedback index was increased in positive and negative directions, reaching a maximum of about 5.8 times the minimum θ error and 2.9 times the minimum $\dot{\theta}$ error at the FF extreme. These same trends also hold true for absolute error rather than percentage error.

To determine whether our results were dependent on a particular choice of parameters, we repeated the hybrid model calculations, systematically varying every nonredundant parameter at least once (see Table 1). We found that, regardless of parameter values, minimum rms errors were achieved with a CFI feedback index of 0. However, the value of that minimum and the relative amount by which it is exceeded using FF or FB were dependent on parameter choices. For example, both the magnitude of minimum error and the relative advantage over FF/FB decreased with increasing damping ratio ζ (see parameter sets b and c). Nevertheless, the sensitivities to parameter choice were quite small overall, with relative advantages over FF ranging from 3.7 to 7.4 in θ and from 1.7 to 3.9 in $\dot{\theta}$ despite parameter changes on the order of twofold or more. The most significant absolute effect was an approximately order of magnitude increase in minimum error (parameter set i), but this occurred when the disturbance covariance was increased by two orders of magnitude, equivalent to a tenfold increase in the rms value of w and therefore indicative of an approximately linear scaling relationship.

5 Discussion

Our results demonstrate the claim that, for dynamical systems subject to both disturbances and measurement noise, there is an optimum level of combined feedforward and feedback that results in better performance than either FF or FB alone. Feedback is a necessary component for any system which must respond to disturbances, and when measurements are accurate, there is no advantage to be gained through feedforward. In the more realistic case where measurements are subject to noise, combining feedforward with feedback can optimally reduce steady-state errors. For example, the results of Fig. 5 showed steady-state errors that were smaller by a factor of about 2 to 7 for a wide range of parameter values.

There were a few anomalies in which the results did not conform to expectations. Estimation theory predicts that errors should increase monotonically towards the FF and FB extremes as the CPG feedback gains decrease or increase, respectively, from their optimal values. In several cases, the FF and FB errors appeared to be lower than expected. Closer examination revealed that errors were magnified by numerical errors when gain values were large or small relative to the integration error tolerance for the simulation. These errors were due to a combination of stiff differential equations and scaling effects in numerical arithmetic, and typically occurred only with a CPG feedback index of ±5. With the exception of these anomalies, all of the results shown in Fig. 5 were consistent with expectations.

We therefore hypothesize that the primary advantage gained by the presence of intrinsic rhythmic oscillations is in the processing of sensory information for use in feedback, rather than to control timing or to sustain a stable limit cycle. Both of these functions are better served through feedback. Strict timing should not in any case be relevant to many rhythmic movements, and even to locomotion. When there is a perturbation to a nominal trajectory, it should be of primary importance to return to the limit cycle in a stable and/or energy-efficient manner rather than to preserve the phasing in place before the perturbation. This expectation has been demonstrated empirically (Kay et al., 1991).

If the purported disadvantages of feedforward seem at odds with the prevailing opinion, it is in part because this term is technically not appropriate for biological CPGs under the influence of feedback. In standard control terminology, the hybrid FF/FB model (Fig. 4) is a closed-loop feedback system, no component of which could be considered feedforward. This is true despite the fact that it will generate rhythmic output even in the absence of the error signal e. CPG behavior arises from

Fig. 6. Steady-state position and velocity errors for hybrid system using variety of parameter sets. **a.** Position errors were minimized for feedback gain index of 0, using all parameter sets. **b.** Velocity errors were either minimized, or within 1% of minimum, for feedback gain index of 0, using all parameter sets. Results demonstrate general principle of hybrid FF/FB control: steady-state error is minimized for some intermediate value of CPG feedback gain, regardless of parameter choice.

a. Parameter Sensitivity: Position Error

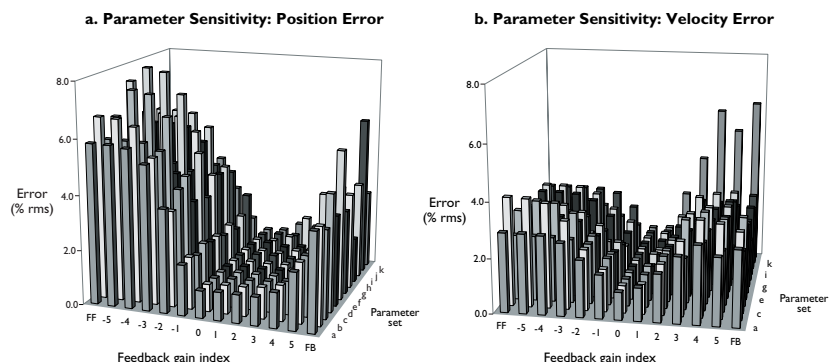b. Parameter Sensitivity: Velocity Error

Table 1. Effect of parameter variations on CPG feedback gains and steady-state rms error. For each parameter set, the name of the parameter and its perturbed value is given, along with values for two feedback gains and two sets of rms error. Each set contains one column for rms error in θ or $\dot{\theta}$, followed by two columns containing the factor by which this error is multiplied under pure feedforward and pure feedback, respectively.

Set	Parameter	Value	L_{11}	L_{22}	θ rms error			$\dot{\theta}$ rms error		
					optimal	FF	FB	optimal	FF	FB
a	all	—	1.02	3.88	1.4%	5.8	3.6	1.7%	2.9	2.7
b	ζ	0.025	0.88	2.32	2.0%	6.6	3.5	2.2%	3.9	3.1
c	ζ	0.4	1.11	7.00	1.1%	5.7	3.2	1.1%	2.4	2.3
d	α	0.2	0.98	4.38	1.5%	6.4	4.3	1.3%	3.1	3.2
e	α	0.4	0.93	3.04	1.5%	4.5	3.3	2.1%	2.6	2.7
f	U	1	1.01	6.82	1.1%	7.4	5.5	0.9%	2.8	2.6
g	U	0.25	0.91	2.90	1.5%	4.3	3.1	2.3%	2.5	2.5
h	K	0.6	1.05	3.72	1.3%	6.0	3.5	3.0%	1.7	1.6
i	w	×100	1.12	3.90	12.8%	5.5	1.7	17.1%	2.9	2.6
j	w_2	×100	1.07	3.88	1.4%	5.9	3.6	1.7%	2.9	2.4
k	v_1	×10	0.28	3.98	2.2%	3.7	5.9	1.8%	2.7	2.7
l	v_2	×10	2.10	0.79	1.9%	4.2	2.9	2.4%	2.0	6.2

two components of the model: an internal model that can be used for state estimation in any type of movement (including posture or non-rhythmic movement), and a feedback gain K that can stabilize posture or produce rhythmic movement depending on its magnitude. In the case of zero CPG feedback ($L=0$) there is a sudden change in terminology; the internal model becomes a feedforward controller and the control feedback gain K becomes a feedforward gain. Because most CPGs have feedback pathways, it is perhaps more appropriate to think of intrinsic CPG oscillations in a feedback rather than feedforward context. Cohen (1992) proposes the term "heterarchical control" for this type of interaction; the internal model hypothesis considers the CPG to be a sensory processor within the feedback loop.

Although the hypothesis has been studied using a very simple model, experience suggests that it is applicable to a wide variety of more complex systems. The conditions under which the output of a constant-gain state estimator (13)-(14) serves as an appropriate feedback control signal are theoretically limited to stationary linear systems. However, practically speaking, the constant gain estimator appears to be applicable to situations such as the HFB system used here.

The model studied here is restricted to rhythmic limb motion, but may have some relevance to locomotion as well. The stance phase of locomotion certainly does not resemble the motion of a simple pendulum, but its inverted pendulum behavior is also rhythmic. It is reasonable to suppose that the propulsive extension of the stance leg which occurs just prior to toe-off (Donelan et al., 2001 in press) can advantageously be generated through feedback. Again, the advantage of

feedback is that the timing is adjusted based on the actual state of the limb, and the disadvantage is a sensitivity to sensory errors. Just as with the present model, a state estimator can optimally combine the advantages of feedback and a feedforward internal model. Finally, motion of the swing leg can be modeled as a pendulum-like oscillation forced by actively applied muscle torques (Kuo, 2001), very similar to the model presented here.

Applying the hypothesis to other systems leads to interesting conceptual predictions. For example, for systems with multiple body or limb segments, the state estimation hypothesis predicts the presence of multiple CPGs and bi-directional feedback paths which most heavily weight neighboring segments. Intersegmental coupling of this sort has been identified in the lamprey. Comparative tests are possible based on scaling laws. Internal models are only advantageous for dynamical systems, and limb dynamics are expected to be most significant for larger animals. Animals with small limbs are more likely to move in an overdamped environment in which dynamics are less significant. In this situation, motor commands may act more as position commands rather than force commands, and the limbs may be largely stabilized by mechanical, rather than sensory, feedback. Sensory feedback should therefore be less of an issue for very small animals.

Other tests of the hypothesis may be possible if there is a degree of feedback connection plasticity. If an animal actively adjusts feedback weights based on the efficacy (and therefore the precision) of sensory information, then the state estimation hypothesis predicts that artificial corruption of a sensory signal should result in a decrease in its weight. Such a test

would require a means to substitute or augment the information carried by an afferent.

Finally, it should be emphasized that the hybrid model studied here should be taken conceptually rather than literally. It uses efference copy and sensory error signals to drive an internal model without specifying the particular anatomical structure for these components. There are many possible schemes based on half-center, pacemaker flexor burst generators, or other networks (Pearson, 1976) that can perform the function of an internal model, and these networks could encode information through either spiking or nonspiking neurons (Pearson and Fourtner, 1975). Although mammalian α-γ coactivation is used to generate sensory error signals in the model of Fig. 4, there are analogous methods employed in other vertebrates (Vinay et al., 1996) and even invertebrates (Cohen, 1992). The internal model hypothesis has few anatomical constraints beyond specifying the necessity of such signals and providing a conceptual framework for how and why they are processed. In fact, there is evidence that state estimation is applied at higher levels of the CNS for motor planning (Wolpert et al., 1995). Its main purpose is to provide a conceptual basis for interpreting and identifying common functions among the disparate anatomies of a wide variety of species generating rhythmic movements.

References

Alexander RM (1989) Optimization and gaits in the locomotion of vertebrates. Physiol Rev 69: 1199-1227

Baev KV, Esipenko VB, Shimansky YP (1991) Afferent control of central pattern generators: experimental analysis of scratching in the decerebrate cat. Neurosci 40: 239-256

Brown TG (1914) On the nature of the fundamental activity of the nervous centres, together with an analysis of the conditioning of rhythmic activity in progression, and a theory of evolution of function in the nervous system. J Physiol (Lond) 48: 18-46

Bryson AE, Ho YC (1975) Applied Optimal Control. Hemisphere, Washington DC

Cohen AH (1992) The role of heterarchical control in the evolution of central pattern generators. Brain Behav Evol 40: 112-124

Donelan JM, Kram R, Kuo AD (2001) Simultaneous positive and negative external mechanical work in human walking. J Biomech In press

Gray J (1950) Physiological mechanisms in animal behavior. Cambridge University Press, Cambridge

Grillner S, McClellan A, Perret C (1981) Entrainment of the spinal pattern generators for swimming by mechanosensitive elements in the lamprey spinal cord in vitro. Brain Res 217: 380-386

Grillner S, Wallén P (1985) Central pattern generators for locomotion, with special reference to vertebrates. Annu Rev Neurosci 8: 233-261

Guckenheimer J, Holmes P (1983) Nonlinear oscillations, dynamical systems, and bifurcations of vector fields. Springer-Verlag, New York

Hatsopoulos N (1996) Coupling the neural and physical dynamics in rhythmic movements. Neural Computation 8: 567-581, 1996

Kay BA, Saltzman EL, Kelso JA (1991) Steady-state and perturbed rhythmical movements: a dynamical analysis. J Exp Psych: Hum Percept & Perf 17: 183-197

Kuo AD (2001) A simple model predicts the preferred speed-step length relationship in human walking. ASME J Biomech Eng 123: 264-269

McGeer T (1993) Dynamics and control of bipedal locomotion. J theor Biol 163: 277-314

Mellen N, Kiemel T, Cohen AH (1995) Correlational analysis of fictive swimming in the lamprey reveals strong functional intersegmental coupling. J Neurophysiol 73: 1020-1030

Pearson KG (1976) The control of walking. Sci Am 235: 72-86

Pearson KG, Fourtner CR (1975) Nonspiking interneurons in walking system of the cockroach. J Neurophysiol 38: 33-52

Raibert MH (1986) Legged robots that balance. MIT Press, Cambridge

Shik ML, Severin FV, Orlovsky GN (1966) Control of walking and running by means of electric stimulation of the midbrain. Biofizika 11: 659-666

Vinay L, Barthe J-Y, Grillner S (1996) Central modulation of stretch receptor neurons during fictive locomotion in lamprey. J Neurophysiol 76: 1224-1235

Wolpert DM, Ghahramani Z, Jordan MI. An internal model for sensorimotor integration. Science 269: 1880-1882